CORRIDOR FOLLOWING BASED ON THE FUSION OF REDUNDANT CONTROL SIGNALS

EDUARDO FREIRE[1], CARLOS SÓRIA[2], RICARDO CARELLI[2]

[1]*Núcleo de Engenharia Elétrica – Centro de Ciências Exatas e Tecnologia – Universidade Federal de Sergipe*
Av. Marechal Rondon, S/N, Jardim Rosa Elze, São Cristovão-SE, CEP 49100-000, Brasil
[2]*Instituto de Automática – Universidad Nacional de San Jaun*
Av. San Martín Oeste, 5400 San Juan, Argentina
E-mails: efreire@ufs.br, csoria@inaut.unsj.edu.ar, rcarelli@inaut.unsj.edu.ar

Abstract— This work presents a control strategy for mobile robots navigating in corridors, using the fusion of the control signals from two instances of the same controller: one is based on the perspective lines of the corridor (the projection of lines formed by the intersection of the walls and the floor) and the other is based on distance measurements performed by ultrasonic sensors. Both controllers generate angular velocity commands to keep the robot navigating along the corridor, and compensate for the dynamics of the robot. The fusion of both control signals is made using a Decentralized Information Filter - DIF. Experiments on a laboratory robot are presented to show the feasibility and performance of the proposed controller.

Keywords— Control Fusion, Corridor Navigation, Stability, Redundant Controllers.

1 Introduction

A main characteristic of Autonomous Navigation is the capability of capturing environmental information through external sensors, such as vision, distance or proximity sensors. Although distance sensors (e.g., ultrasound and laser types), which detect and measure distances to walls and obstacles near the robot, are the most commonly used sensors, vision sensors are increasingly being used due to their capability to provide more information about the environment.

When autonomous mobile robots navigate within indoor environments (e.g., public buildings or industrial facilities) they should be able to move along corridors, turn at corners and enter and maneuver into the rooms. Regarding motion along corridors, some control algorithms have been proposed in various works. In (Bemporad, *et al.*, 1997), a globally stable control algorithm for wall-following based on incremental encoders and one sonar sensor is developed. In (Vasallo *et al.*, 1998), image processing is used to detect perspective lines and to guide the robot following the corridor centerline. This work assumes an elementary control law and does not prove control stability. In (Yang, Tsai, 1999), ceiling perspective lines are employed for robot guidance, but it also lacks a demonstration on system stability. Other authors proposed techniques for using optical flow for corridor centerline guidance. Some approaches incorporate two video cameras on the robot sides, and the optical flow is computed by comparing the apparent velocity of image patterns from both cameras (Santos-Victor *et al.*, 1995). In (Dev *et al.*, 1997b), a camera is used to guide a robot along a corridor centerline or to follow a wall. In (Servic *et al.*, 2001) perspective lines are used to find the absolute orientation within a corridor. In (Carelli *et al.*, 2002) the authors have proposed the fusion of the outputs of two vision-based controllers using a Kalman Filter in order to guide the robot along the centerline of a corridor. One of the controllers is based on optical flow, and the other is based on the perspective lines of the corridor. This work presents a stability analysis for the proposed control system.

In general, the works previously cited have not included a stability analysis of the control system. But, even if a control system is stable, there is still a possibility that it would not be able to attain its control objective. This is due to the fact that a control system is able to work properly only if its state variables can be correctly measured in time. In many situations the state variables are not available due to environment conditions such as illumination, surface textures, perturbations from image quality loss, and other factors. A useful approach to increase the robustness of a control system is to use data from several sources to estimate its state variables.

Excepting for a few cases, as in (Bemporad *et al*, 1997), and (Carelli *et al*, 2002), these works do not present a stability analysis for the control system. On the other hand, the performance of the control system depends on environment conditions such as illumination, surface textures, perturbations from image quality loss, and other factors, all of which prevents each individual controller from achieving acceptable robustness properties. A solution for this problem is to consider multiple controllers, based on different sensing information, which operate simultaneously. Although having the same control objective, the controllers can be coordinated using the concept of behavior coordination (Khalil, 1996). Within this concept, the command fusion schemes accept a set of behavior instances that share the control of the whole system at all times.

Command fusion schemes can be classified into four categories: voting (e.g. DAMN, Rosenblat, 1997), superposition (e.g. AuRA, Arkin and Balch, 1997), Multiple Objective (e.g. Multiple Decision-Making Control, Pirjanian, 2000) and fuzzy logic (e.g. Multivaluated Logic Approach, Saffiotti *et al*, 1995). Another example of a command fusion strategy is the dynamic approach to behavior-based robotics, (Bicho, 1999). In this paper we consider the command fusion structure previously proposed in Freire *et al*, 2004.

In this work, two instances of the same controller are used. Both instances use the same state variables: $\tilde{x}(t)$ (the distance from the robot center to the corridor centerline) and $\theta(t)$ (the angle between the robot heading and the corridor orientation) and produce as output signal an angular velocity. The state variables to the first controller are calculated based on the perspective lines of the corridor (the projection of lines formed by the intersection of the walls and the floor). The position of these lines on the image plane allows for calculation of the distance and orientation of the robot with respect to the corridor centerline. The second instance of the controller uses distance measurements performed by ultrasonic sensors to calculate its state variables. The obtained results show that controllers based on absolutely different sensory information, but with the same control objective, can be fused to accomplish a task. The linear speed of the robot was kept constant. Both controllers are redundant, because they have the same control objective. They are based, however, in different kinds of information. Here, we propose a fusion of both commands to attain a control signal that allows for robust navigation along corridors. For the fusion, the control architecture via control output fusion is used, as proposed in Freire *et al*. (2004), employing a Decentralized Information Filter that minimizes the uncertainty level in both controllers. This uncertainty is evaluated in terms of the sensing error and the environment conditions by means of a covariance function for each controller. A stability analysis of the resulting control system is presented as well. The work also presents experimental results on a Pioneer 2DX robot navigating at the Institute of Automatics (INAUT), National University of San Juan (UNSJ), Argentina.

2 Robot and Camera Models

2.1 Robot Model

Fig. 1 represents the coordinate systems associated with the robot and the environment: a world system [W], a platform system [R] fixed to the robot and a sensor system [C] fixed to the vision camera. Regarding Fig. 1, the kinematics model of a unicycle type robot can be expressed as (Dev *et al*, 1997a),

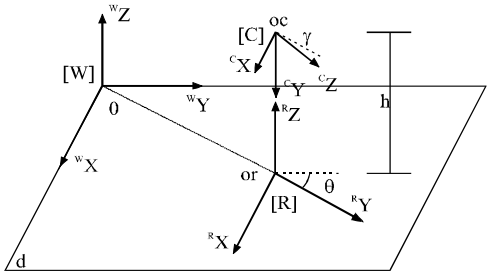

Figure 1. Coordinate systems.

$$\begin{cases} \dot{y} = v \cdot \cos(\theta) \\ \dot{x} = v \cdot \sin(\theta) \\ \dot{\theta} = \omega \end{cases} \quad (1)$$

where ω is the angular velocity and v the linear velocity of the robot, $x \equiv {}^{W}x_{or}$, $y \equiv {}^{W}y_{or}$.

In order to compensate for the dynamics of the robot, a dynamic model was obtained experimentally.

Of particular interest is the model relating $\omega_r \rightarrow \omega_y$, where ω_r is the reference angular velocity sent to the robot, and ω_y is the measured angular velocity of the robot. A second order system approximately represents the identified model,

$$\omega = \frac{k_\omega a_\omega}{s^2 + b_\omega s + a_\omega} \omega_r \quad (2)$$

with $k_\omega = 0.45$, $a_\omega = 104.6$ and $b_\omega = 9.21$.

2.2 Camera Model

A pinhole model of the camera is considered. The following relationship can be obtained from Fig. 2,

$$r = \alpha \lambda \frac{p}{{}^{c}p_z} \quad (3)$$

where r is the projection of a point P on the image plane, λ is the focal length of the camera, α is a scale factor, and ${}^{c}p_z$ is the depth coordinate.

2.3 Differential Camera-Robot Model

This subsection presents the kinematics relationship of the camera mounted on the moving robot evolving with linear velocity v and angular velocity ω. The Coriolis equation renders the motion of a point P in a coordinate system with translational and rotational motion V and Ω,

$$\dot{P} = -V - \Omega \times P \quad (4)$$

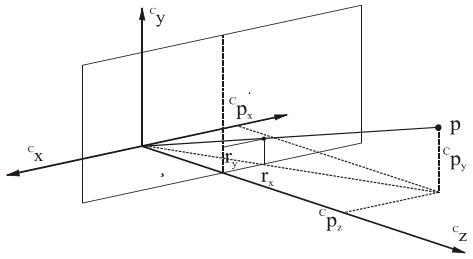

Figure 2. Perspective projection camera model.

By differentiating (3) with respect to time and using both (4) and (3), the components of $\dot{r}$ on the image plane are found as,

$$\dot{r}_x = \frac{-\lambda V_x + r_x V_z}{P_z} + \frac{\omega_x}{\lambda} r_x r_y - \omega_y(\lambda + \frac{r_x^2}{\lambda}) - \omega_z r_y \quad (5)$$

$$\dot{r}_y = \frac{-\lambda V_y + r_y V_z}{P_z} + \omega_x(\lambda + \frac{r_y^2}{\lambda}) - \frac{\omega_y}{\lambda} r_x r_y - \omega_z r_x \quad (6)$$

For the camera mounted on the robot's center and pointing forward, $V_x = V_y = 0$ and $\omega_x = \omega_z = 0$. Further, by calling $v = V_z$, $\omega = \omega_y$, (5) and (6) can be written as,

$$\dot{r}_x = \frac{r_x v}{{}^c p_z} - \omega\left(\lambda + \frac{r_x^2}{\lambda}\right) \quad \dot{r}_y = \frac{r_y v}{{}^c p_z} - \frac{\omega}{\lambda}\left(r_x r_y\right) \quad (7)$$

which represent the differential kinematics equations for the camera mounted on the robot.

2.4 Model for the perspective lines

The position and orientation of the robot can be obtained from the projection of the perspective lines in the corridor on the image plane. The parallel lines resulting from the intersection of corridor walls and floor are projected onto the image plane as two lines intersecting at the so-called vanishing point.

A point P in the global frame [W] can be expressed in the camera frame [C] as,

$${}^C p = {}^C R_W ({}^W p - {}^W p_{or}) - {}^C R_R \, {}^R p_{oc}$$

where

$${}^C R_R = \begin{bmatrix} 1 & 0 & 0 \\ 0 & -\sin(\gamma) & -\cos(\gamma) \\ 0 & \cos(\gamma) & -\sin(\gamma) \end{bmatrix},$$

$${}^C R_W = \begin{bmatrix} \cos(\theta) & -\sin(\theta) & 0 \\ -\sin(\theta)\sin(\gamma) & -\cos(\theta)\sin(\gamma) & -\cos(\gamma) \\ \sin(\theta)\cos(\gamma) & \cos(\theta)\cos(\gamma) & -\sin(\gamma) \end{bmatrix}.$$

with γ the camera tilt angle and θ the robot heading.

Considering the component-wise expressions for the pinhole camera model (3),

$$r_x = \alpha_x \lambda \frac{{}^C p_x}{{}^C p_z}, \quad r_y = \alpha_y \lambda \frac{{}^C p_y}{{}^C p_z} \quad (8)$$

any point in the global coordinate system is represented in the image plane as a projection point with coordinates

$$r_x = \alpha_y \lambda \frac{A\cos(\theta) - B\sin(\theta)}{C} \quad (9)$$

$$r_y = \alpha_y \lambda \frac{-A\sin(\theta)\sin(\gamma) - B\cos(\theta)\sin(\gamma) - \cos(\gamma)h}{C} \quad (10)$$

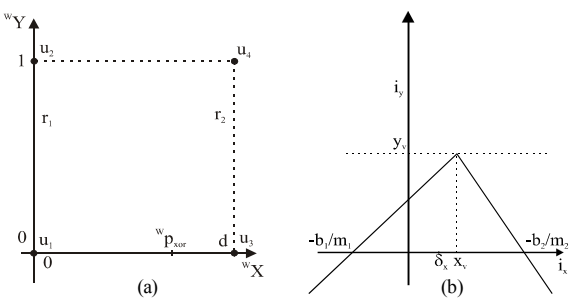

Figure 3. a) Guide lines in the corridor b) Perspective lines.

where

$$A = \left({}^W p_x - {}^W p_{xor}\right), \quad B = \left({}^W p_y - {}^W p_{yor}\right)$$

$$C = \sin(\theta)\cos(\gamma)A + \cos(\theta)\sin(\gamma)B - \sin(\gamma)h$$

Now consider the points $u_1 = [0 \;\; 0 \;\; 0]^T$, $u_2 = [0 \;\; 1 \;\; 0]^T$, $u_3 = [d \;\; 0 \;\; 0]^T$, $u_4 = [d \;\; 1 \;\; 0]^T$ that define the intersection lines $r_1 = (u_1, u_2)$ and $r_2 = (u_3, u_4)$ between corridor walls and floor, as illustrated in Fig. 3a. Based on (9) and (10), the following relationships are obtained for the slope of the perspective lines, the vanishing point coordinates and the intersection of both lines with the horizontal axis in the image plane, (see Fig. 3b).

$$m_1 = \frac{\alpha_y}{\alpha_x} \frac{h\cos(\theta)}{(\cos(\gamma){}^W p_{xor} + \sin(\theta)\sin(\gamma)h)} \quad (11)$$

$$m_2 = \frac{\alpha_y}{\alpha_x} \frac{h\cos(\theta)}{(\cos(\gamma)({}^W p_{xor} - d) + \sin(\theta)\sin(\gamma)h)} \quad (12)$$

$$x_v = -\frac{\alpha_x \lambda \tan(\theta)}{\cos(\gamma)} \quad (13)$$

$$y_v = \alpha_y \lambda \tan(\gamma) \quad (14)$$

$$\frac{b_1}{m_1} = \frac{\alpha_x \lambda(\sin(\theta)\cos(\gamma)h - {}^W p_{xor}\sin(\gamma))}{h\cos(\theta)} \quad (15)$$

$$\frac{b_2}{m_2} = \alpha_x \lambda \frac{(d - {}^W p_{xor})\sin(\gamma) + h\sin(\theta)\cos(\gamma)}{h\cos(\theta)} \quad (16)$$

3 Data from Vision Sensor

It is important to express the control objective of navigating along the corridor centerline in terms of the image features from perspective lines. The robot follows the centerline of the corridor when the slope of both perspective lines becomes equal; that is, when x_v (the vanishing point) and δ_x (the middle point between the intersection of both perspective lines with the horizontal axis) are equal to zero (see Fig. 3b). In the workspace, orientation error θ and position error relative to the center of the corridor $\tilde{x} = {}^W p_{xor} - d/2$ are defined. These errors can be expressed in terms of the image features x_v and δ_x. Equation (13) can be written as,

$$x_v = K_1 tan(\theta), \quad K_1 = -\frac{\alpha_x \lambda}{\cos(\gamma)}$$

from which,

$$\theta = arctan\left(\frac{x_v}{K_1}\right) \quad (17)$$

Additionally,

$$\delta_x = -\frac{1}{2}\left(\frac{b_1}{m_1} + \frac{b_2}{m_2}\right)$$

By substituting (15) and (16),

$$\delta_x = -\alpha_x \lambda \frac{h sin(\theta)\cos(\gamma) - sin(\gamma)({}^W p_{xor} - d/2)}{h\cos(\theta)}$$

and recalling that $\tilde{x} = {}^W p_{xor} - d/2$, $\tilde{x}$ can be explicitly expressed as

$$\tilde{x} = \frac{\cos(\theta)}{K_2}\left(\delta_x - K_3 \, tan(\theta)\right) \quad (18)$$

where $K_2 = \alpha_x \lambda \frac{sin(\gamma)}{h}$, $K_3 = -\alpha_x \lambda \cos(\gamma)$.

Eqs. (17) and (18) render the orientation and position errors as a function of x_v and δ_x.

4 Data from Ultrasonic Sensors

The controller based on the position of the robot with respect to the centerline of the corridor requires the values of states $\tilde{x}(t)$ and $\theta(t)$ at each instant. These values can be obtained from sonar measurements. Fig. 4 shows a typical situation where lateral sonar sensors S_0, S_{15}, S_7, and S_8 are used.

For this case, the following equations allow calculating the state variables,

$$dleft = \frac{y_{S0} + y_{S15}}{2}; \quad dright = \frac{y_{S7} + y_{S8}}{2} \tag{19}$$

$$diff = \frac{(y_{S15} - y_{S0}) + (y_{S7} - y_{S8})}{2} \tag{20}$$

$$\theta = \sin^{-1}\left(\frac{diff}{d}\right); \quad \tilde{x} = \frac{(dright - dleft)}{2} \tag{21}$$

Sonar measurements may deteriorate or be impossible to obtain under certain circumstances as, for example, when the robot is traveling close to an open door in the corridor, or when the robot has a significant angle of deviation from the corridor axis. The latter condition originates from the fact that a sonar sensor collects useful data only when its direction orthogonal to the reflecting surface lies within the beam width of the receiver, thus allowing for wall detection only for a restricted heading range (Bemporad *et al*, 1997). The range for this angle is approximately φ = 17º for the electrostatic sensors in the robot used in the experiences. On this account, it is important to consider other measurements as well, such as the odometric data provided by the robot. The fusion of these data using optimal filters produces optimal estimations of the robot states, thus minimizing the uncertainty in the sensor measurements. Some authors, as in Sasiadek and Hartana (2000), have fused the odometric and sonar data. In this work we used an Extended Information Filter, (Mutambara, 1998), to estimate the values of states $\tilde{x}(t)$ and $\theta(t)$ based on the observations made by the ultrasonic sensors (eq. 21), and also based on the odometric data.

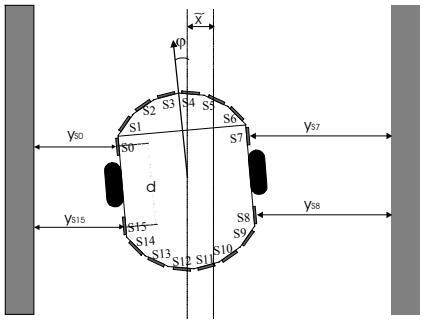

Figure 4: Calculation of state variables using ultrasonic sensors.

5 Controller Based on the Robot Posture with Respect to the Centerline of the Corridor

This section presents the design of the controller. Multiple instances of the controller produce output signals, which will be fused to control the mobile robot navigation along the corridor.

The design objective is to obtain a controller which, based on estimated values of the state variables θ and $\tilde{x}$ obtained from data fusion, attains

$$\lim_{t\to\infty}\begin{pmatrix}\tilde{x}(t)\\ y(t)\end{pmatrix} = \begin{pmatrix}0\\ \int v.dt + y(0)\end{pmatrix}$$

that is, the control navigation objective is asymptotically obtained. To this aim, the following control law is proposed

$$\omega_d = -K_{s\theta}(\theta)\,\theta - K_{s\tilde{x}}(\tilde{x})\,\tilde{x}\,v\,\frac{\sin(\theta)}{\theta} \tag{22}$$

v = constant

where $K_{s\theta}(\theta)$ and $K_{s\tilde{x}}(\tilde{x})$ are variables designed to avoid saturation of control signals.

By considering (1) and (22) with state variables θ and $\tilde{x}$, the unique equilibrium point of the closed loop equation is at $[0 \quad 0]^T$. Regarding the following Lyapunov function can prove asymptotic stability of the control system

$$V(\tilde{x},\theta) = \frac{\theta^2}{2} + \int_0^{\tilde{x}} K_{s\tilde{x}}(\eta)d\eta$$

and by applying the Krasovskii-Lasalle theorem (Khalil, 1996). Saturation gains in (22) can be defined as follows (Carelli, Freire, 2003),

$K_{s\theta}(\theta) = \frac{K_{s1}}{a_1 + |\theta|}$, where $K_{s1} > 0$ and $a_1 > 0$, in order to obtain a positive definite function. Doing likewise with, $K_{s\tilde{x}}(\tilde{x}) = \frac{K_{s2}}{a_2 + |\tilde{x}|}$, with $K_{s2} > 0$, $a_2 > 0$.

The constants are selected such that the terms in (22) do not saturate of the control signal ω_d. Considering the dynamic model of the robot (2),

$$\ddot{\omega} + b_\omega \dot{\omega} + a_\omega \omega = k_\omega a_\omega \omega_r \tag{23}$$

an inverse dynamics control law is regarded

$$\omega_r = \frac{1}{k_\omega a_\omega}\{\eta + b_\omega \dot{\omega} + a_\omega \omega\} \tag{24}$$

where η is a variable defined as,

$$\eta = \ddot{\omega}_d + k_{d\omega}\dot{\tilde{\omega}} + k_{p\omega}\tilde{\omega} \tag{25}$$

$$\tilde{\omega} = \omega_d - \omega$$

In (25), ω_d is given by (22). Besides, $k_{p\omega}$, $k_{d\omega}$, are design gains.

The closed loop equation to allow the exactly known of the robot dynamics is given by:

$$\eta = \ddot{\omega}$$

So, replacing the value of η in the control law (25) results in:

$$\ddot{\tilde{\omega}} + k_d\dot{\tilde{\omega}} + k_p\tilde{\omega} = 0$$

Which implies $\tilde{\omega}(t) \to 0$ when $t \to \infty$.

6 The Control Fusion Process

The control system is based on the fusion of control signals produced by two instances of the same controller, each one working using state variables obtained in a different way. The control output signal fusion scheme is based on the decentralized information filter, as presented in Fig. 5. It is assumed that the system and the measurement noises are white and uncorrelated. The reasons to select a decentralized version of the information filter instead of a classic Kalman filter can be found in (Freire *et al*, 2004), and were not presented here due to the limited space available. The variables y and Y that appear in Fig. 5 are respectively the information vector and the information matrix. The information matrix is the inverse of the covariance matrix P of the Kalman filter and the vector of information is obtained by multiplying the information matrix by the state vector. More information about the DIF is given in (Freire *et al*, 2004). The variance assigned to each controller is the variance of its output signal, which is recursively calculated using:

$$\bar{x}(k) = \bar{x}(k-1) + k \cdot (x(k) - \bar{x}(k-1))$$

$$\mathrm{var}(x(k)) = \mathrm{var}(x(k-1)) + k \cdot \left[(x(k) - \bar{x}(k-1))^2 - \mathrm{var}(x(k-1)) \right]$$

where k is the forgetfulness factor.

Such control system is able to work in static and dynamic environments. Even thought that the two controllers presented in Fig. 5 are two instances of the same controller, they may produce conflicting or contradictory outputs. The system is able to deal with these cases, since the existence of contradictory or conflicting information is in the essence of data or command fusion schemes. The assigned variance to each controller should reflect the confidence of the state variables available. So, the output of the fusion scheme tends to the output of the controller with the smallest variance. The stability of a control system based on the fusion of control signals from homogeneous or redundant controllers using Kalman and Information filter was analyzed in Carelli *et al* (2002) and Soria *et al* (2006), respectively. It was found that such systems are ultimately bounded, which means that the ultimate bound on the standard deviation of the error is smaller than that corresponding to errors produced by each controller.

7 Experimental Results

In order to evaluate the performance of the proposed control system, several experiences were done on a Pioneer 2DX robot with an on-board Sony PTZ CCD camera. The images are transmitted via RF to a host computer, where the corridor perspective lines calculation and the ultrasonic data are processed and fused, and the control system is executed. This same computer sends the reference angular and linear velocities to the robot through RF link.

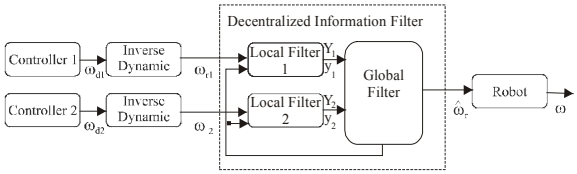

Figure 5: Command fusion scheme.

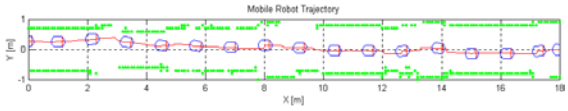

Figure 6: Mobile robot trajectory.

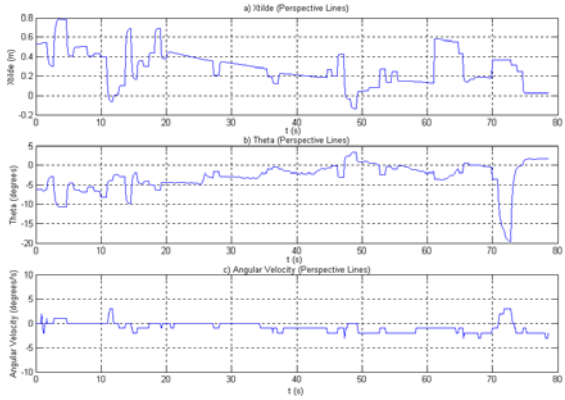

Figure 7: Controller based on perspective lines data.

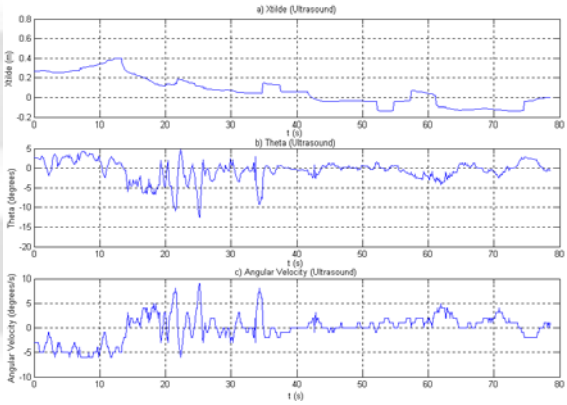

Figure 8: Controller based on ultrasonic distance measurements.

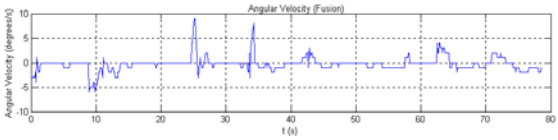

Figure 9: Fused angular velocity.

Fig. 6 shows the trajectory of the robot navigating along a corridor at the INAUT/UNSJ. The experiment is designed in a way that the robot finds different sensing and environment conditions during navigation. The figure shows that the robot is able to follow the corridor centerline, despite of problems like image loss and open doors along the corridor. In Fig. 7, the state variables and control action of the controller based on visual data are presented. Fig. 7a presents an estimate of the state variable $\tilde{x}(t)$, which is obtained using an extended information filter (Mutambara, 1998) and an observation vector formed by the odometric data related to $\tilde{x}(t)$ and the value for $\tilde{x}(t)$ obtained as indicated in eq. 18 (Section 3). The same is valid to Fig. 7b, but in this case

the data is associated to the state variable $\theta(t)$, (eq. 17). In Fig. 7c the control output signal is presented. Fig. 8 has the same structure of Fig. 7, but the information presented is associated with the ultrasonic sensors (eq. 21). The angular velocity resulting from the fusion process is depicted in Fig. 9.

8 Conclusions

This work has presented a control strategy for mobile robots navigating in corridors, using the fusion of control signals from homogeneous controllers. The system was designed to be able to work properly on static or dynamic environments. To this aim two instances of a controller have been used: one based on the perspective lines of the corridor and the other based on distance measurements performed by ultrasonic sensors. Both controllers generate angular velocity commands to keep the robot navigating along the corridor, and to compensate for the dynamics of the robot. The fusion of both control signals is made using a Decentralized Information Filter. The resultant control system is ultimately bounded (Khalil, 1996), as shown in Soria *et al* (2006). Experiments on a laboratory robot have been presented that show the good performance of the proposed controller. Future work includes the fusion of controllers based on other types of external sensors as laser range sensors, for example, and the comparative study of controllers based on data fusion with controllers based on control fusion and with controllers based on both kinds of signal and data fusion.

9 Acknowledgements

The authors gratefully acknowledge SETCIP and CONICET (Argentina), and the UFS (Brazil) for partially funding this research.

10 References

Arkin, R. and T. Balch,. AuRA: principles and practice in review. *Experimental and Theoretical Artificial Intelligence, 9, pp. 175-189* (1997).

Bemporad, R.; Di Marco, M. and Tesi, A. (1997). Wall–following controllers for sonar–based mobile robots. *Proc. 36th. IEEE Conf. on Decision and Control*, San Diego, Dec.

Bicho, E. The dynamic approach to behavior-based robotics. *PhD. Thesis, University of Minho, Portugal* (1999).

Carelli, R. and Freire, E. (2003). Corridor Navigation and Wall-Following Stable Control for Sonar-Based Mobile Robots. *Robotics And Autonomous Systems,* v. 45, p. 235-247.

Carelli, R.; Soria, C.; Nasisi, O. and Freire, E. (2002). Stable AGV Corridor Navigation with Fused Vision-Based Control Signals. *In: IECON'02 – 28º Annual Conference of the IEEE Industrial Electronics Society*, Sevilha. p. 2433-2438.

Dev, A.; Kröse, B. J. A. and Groen, F. C. A. (1997a). Confidence measures for image motion estimation. *RWCP Symposium, Tokio.*

Dev, A.; Kröse, B. and Groen, F. (1997b). Navigation of a mobile robot on the temporal development of the optic flow. *Proc. Of the IEEE/RSJ/GI Int. Conf. On Intelligent Robots and Systems IROS´97*, Grenoble, pp. 558-563.

Dixon, W., D. Dawson, E. Zergeroglu and A Behal. Nonlinear Control of wheeled mobile robots. *Springer Verlag* (2001).

Freire, E.; Bastos-Filho, T.; Sarcinelli-Filho, M. and Carelli, R. (2004). A New Mobile Robot Control Architecture: Fusion of the Output of Distinct Controllers. *IEEE Transactions on Systems Man and Cybernetics Part B-Cybernetics,* v. 34, n. 1, p. 419-429.

Khalil, H. K. (1996). Non-linear systems, Second Edition. *Prentice-Hall.*

Mutambara, A. G. O. (1998). Decentralized Estimation and Control for Multi-sensor Systems. EUA: *CRC Press.*

Pirjanian, P. Multiple objective behavior-based control. *Robotics and Autonomous Systems, 31, pp. 53-60* (2000).

Rosenblatt, J. DAMN: A decentralized architecture for mobile navigation". *PhD Thesis, Carnegie Melon University, USA*. (1997).

Saffiotti, A., K. Konolige and E. Ruspini. A multivaluated logic approach to integrating planning and control. *Artificial Intelligence, 76, pp. 481-526.* (1995).

Santos-Victor, J.; Sandini, G.; Curotto, F. and Garibaldi, S. (1995). Divergent stereo in autonomous navigation: from bees to robots. *Int. Journal of Computers Vision*, 14-159-177.

Sasiadek, J. Z and Hartana, P. (2000). Odometry and sonar data fusion for mobile robot navigation. *6th. IFAC Symposium on Robot Control, SYROCO´00*. Vienna, Austria. Preprints, Vol.II, pp.531-536.

Servic, S. and Ribaric, S. (2001). Determining the Absolute Orientation in a Corridor using Projective Geometry and Active Vision. *IEEE Trans. on Industrial Electronics*, vol. 48, No. 3.

Soria, C. Freire, E. and Carelli, R. (2006). Stable AGV Corridor Navigation Based on Data and Control Signal Fusion. *Latin American Applied Research,* v. 36, n. 2, p. 71-78.

Vassallo, R.; Schneebeli, H. J. and Santos–Victor, J. (1998). Visual navigation: combining visual servoing and appearance based methods. *SIRS´98, Int. Symp. on Intelligent Robotic Systems, Edinburgh, Scotalnd*.

Yang, Z. and Tsai, W. (1999). Viewing corridors as right parallelepipeds for vision-based vehicle localization. *IEEE Trans. on Industrial Electronics*, vol. 46, No. 3.